Proceedings of the 8th International Conference on MicroManufacturing
University of Victoria, Victoria, BC, Canada, March 25-28, 2013

Parametric Studies of Melt Electrospinning Poly ε (caprolactone) Fibers for Tissue Engineering Applications

ICOMM 2013 No.15

Junghyuk Ko[1], Nima K. Mohtaram[2], Patrick C.D. Lee[3], Stephanie M. Willerth[4], and Martin B. Jun[5]
[1] University of Victoria, Mechanical Engineering Department, Canada: jko@uvic.ca
[2] University of Victoria, Mechanical Engineering Department, Canada: nkhadem@uvic.ca
[3] Dow chemical company, 2511 Midlan 433 Building, Midland, MI 48667, US: CDLee@dow.com
[4] University of Victoria, Mechanical Engineering Department & Division of Medical Sciences, Canada: willerth@uvic.ca
[5] University of Victoria, Mechanical Engineering Department, Canada: mbgjun@uvic.ca•

Key Words: melt electrospinning, scaffolds, tissue engineering

ABSTRACT

The process of electrospinning has received remarkable amount of attention as this technique can be used to fabricate suitable scaffolds for cells. In order to control morphology of scaffold, parametric studies are necessary in customized melt electrospinning. In this study, we demonstrate that fiber diameter could be controlled by customized nozzle and parameters which are temperature, voltage, and distance influence to fiber diameter. Moreover, we culture and seed murine CE3 stem cells derived from D3 embryonic stem cell line on fabricated scaffolds. Overall, scaffold controlled by parameter studies holds a promising strategy for superb cell attachment and proliferation.

INTRODUCTION

Most tissue engineering strategies for replacement of functional tissues or organs depend on the application of three dimensional (3D) scaffolds that guide the proliferation and spreading of seeded cells *in vitro* and *in vivo* [1-3]. However, main challenges for tissue engineering applications are fabrication of customized scaffolds for cells. Conventional fabrication methods of such scaffolds have been developed in solvent casting, fiber bonding, phase separation, frozen drying, particulate leaching, and gas foaming [4-9]. However, the methods are difficult to control pore sizes of scaffolds so the scaffolds fabricated by the conventional methods have low gas permeability and porosity.

In recent decades, the process of electrospinning has received remarkable attention due to its ability to fabricate polymer fibers ranging in size from nanometer to micrometer scale in diameter [10]. The introduction of the electric field was able to change the hemispherical liquid drop suspended in equilibrium at the end of needle into Taylor cone. By introducing the electric field, the electric potential balance against the surface tension and viscosity of the polymer solution and polymer melts.

Electrospinning without solvents via the melt may be attracting for biomedical applications such as the tissue engineering of cell constructs where solvent accumulation or toxicity is a worry. Moreover, melt electrospinning is relatively under-studied compared to solution electrospinning but fiber diameter are big from melt electrospinning process, and typical size was reported approximately 100μm [11-17]. Some researchers have tried to reduce fiber diameter using co-polymerization [18] or hybrid process [19, 20].

Superior rheological and viscoelastic polymer have shown their outstanding role in scaffold morphology control since friction from nozzle becomes reduction and polymer comes out uniformly and continuously [21]. We have chosen poly ε-caprolactone (PCL) which is a very common biodegradable polymer approved by U.S. Food and Drug Administration (FDA) for scaffold fabrication. PCL provides a promising platform for the production of longer-term biodegradable and biocompatible scaffolds which may be manipulated physically, chemically and biologically to possess tailorable degradation kinetics to suit a specific anatomic site as reviewed in detail by Woodruff and Hutmacher [22].

In this study, using melt electrospinning we demonstrate that fiber diameter could be successfully controlled by customized nozzle (diameter 150μm to 1.7mm) and significant parameters influenced to fiber diameter also were presented, which are temperature (80°C to 120°C), voltage (10kV to 20kV), and distance (2.5cm and 5cm). Moreover, the diameter of fibers through temperature controlling system is also researched in order to characterize topology of scaffolds, which support tissue ingrowth as well as functionality related to surface affinity and an additional surface area for improved cell attachment and proliferation. Samples are imaged using scanning electron microscopy (SEM) In addition, we culture and seed murine CE3 stem cells derived from D3 embryonic stem cell line, on the sterilized and punched scaffolds. Viability and growth of CE3 are also assayed to demonstrate the survival of the seeded cells on the electrospun microfibers.

MATERIALS AND METHOD

A. MATREIALS

PCL's (Mn = 45,000, Sigma Aldrich, USA) melting point is approximately 60°C. The experiments are conducted at various temperatures using temperature control system. During the melt electrospinning process, 20kV was applied to the melt PCL using a high voltage power supply (Gamma High Voltage Research Inc., USA) and the working distance be-

• corresponding author

tween the nozzle and aluminum foil collector was 5cm. The PCL granules were dispensed into melting chamber with the nozzle attached and then heated to the desired temperature. The temperature-equilibrated PCL polymer was then extruded by electric force with the help of gravity and syringe pump at a controlled speed, counter balancing viscosity and surface tension. As shown in Fig. 1, the zero shear rate viscosity of PCL was measured by ARES-G2 rheometer (TA Instruments, USA) as 291.5Pa*Sec. at 80°C using 25mm parallel plates geometry with the gap of 25mm. For the collection of controlled-microfiber scaffolds, a wood plate covered with aluminum foil served as the counter electrode.

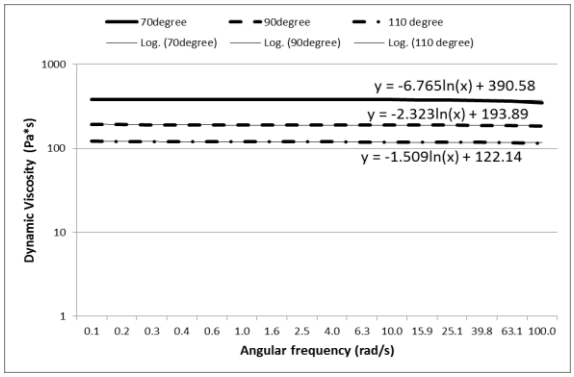

Fig. 1 Rheology data of PCL (Mn=45,000)

B. MELT ELECTROSPINNING SETUP

A custom-made melt electrospinning apparatus was built as shown in Fig. 2(A). The melt electrospinning apparatus consisted of CNC machine (K2 CNC Inc., USA), custom-made chamber press, syringe pump (New Era Pump Systems Inc., USA), heating band (Orion telescopes Inc., USA), custom-made machined melting chamber, custom-made collecting drum, and the custom-made nozzles which could be interchanged. Fig. 2(B) shows effective heating and cooling in thermal simulation of melt electrospinning setup. Initial temperature, heat power and convection respectively sets to 20°C on all exposed faces, 40W on exposed faces of heating pad and 25W/m^2 on all exposed faces. The flat tipped nozzles used to extrude the melt were custom-made from aluminum 6061 with internal diameters ranging from 150 µM to 1.7 mm as shown in Fig. 3(A). The custom-made nozzle was machined using conventional lathe machine and then the nozzle hole was fabricated by femtosecond laser pulse ablation. The femtosecond laser system (Spectra-Physics) was operating at 800 nm with a pulse duration of 120 fs and repetition rate of 1 kHz during the fabrication process. The irradiation power used in machining the nozzles was 300 mW at a beam diameter of 3 mm. The beam was focused through a 20X microscope objective lens (Mitutoyo company) with a numerical aperture of 0.4. As shown in the Fig. 3(B) and (C), the motion of the sample stage followed a helical path (generated using the software, GOL3D (JPG Micro Services and GBC&S)) to ablate material from the nozzle head and cut a circular hole.

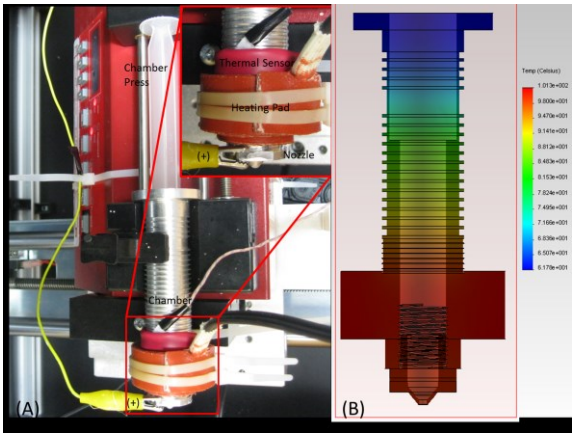

Fig. 2 (A) Cutstom-built melt electrospinning device setup. This device consisted of chamber press, CNC machine, syringe pump, melting chamber, heating pad, and machined nozzle, (B)Thermal simulation result using Solidworks 2011.

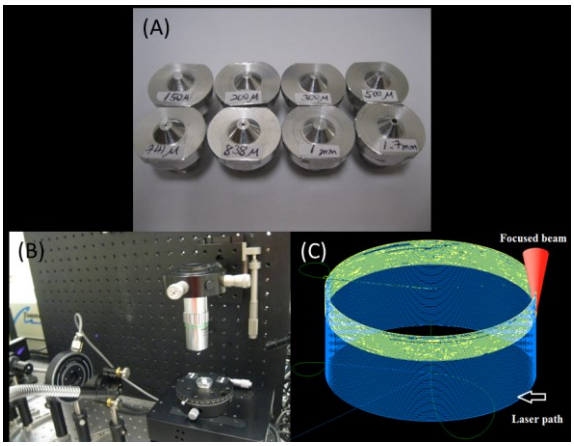

Fig. 3 (A) completed machined nozzles (B) Femtosecond laser system setup consists of microscope objective lens, 4-axis translation stage, and shutter, (C) Helical tool path generated using GOL3D to drill a hole at center of the surface on the machined nozzle

C. TEMPERATURE CONTROL SYSTEM

In order to control temperature in chamber, Proportional-Integral-Derivative (PID) controller was used in Fig. 4. The differences between filtered thermal data from thermometer and desired temperature are implanted to the PID controller and calculated voltage signals are converted with voltage by Arduino control board. Gains for PID are respectively 300, 10 and 50 achieved through repetitive trying.

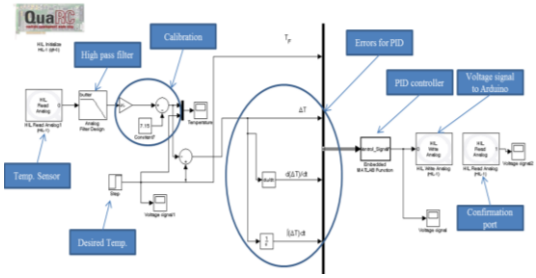

Fig. 4 Schematic of control algorithm in Matlab Simulink

The main command and communication module, which directs all control experiments, was implemented in Matlab/Simulink interfaced with QuaRC rapid control prototyping software from Quanser Consulting Inc. An 8-channel Q8 hardware-in-the-loop control board (also from Quanser) was used to interface between the host PC and the heating pad. In Fig. 5, a schematic diagram of the overall temperature control system is represented. As shown in Fig. 6, it is possible to monitor and control temperatures using voltage signals in real time with this system. The main purpose of using this system is to monitor the temperatures in real time since temperature is the significant parameter for melt electrospinning.

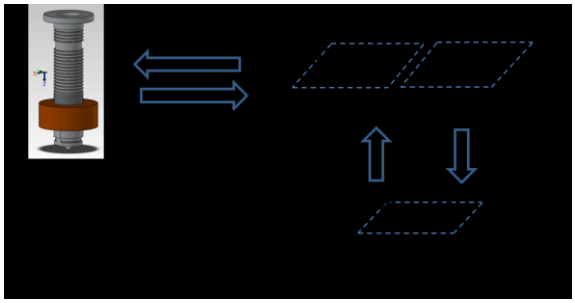

Fig. 5 Schematic of overall temperature control system

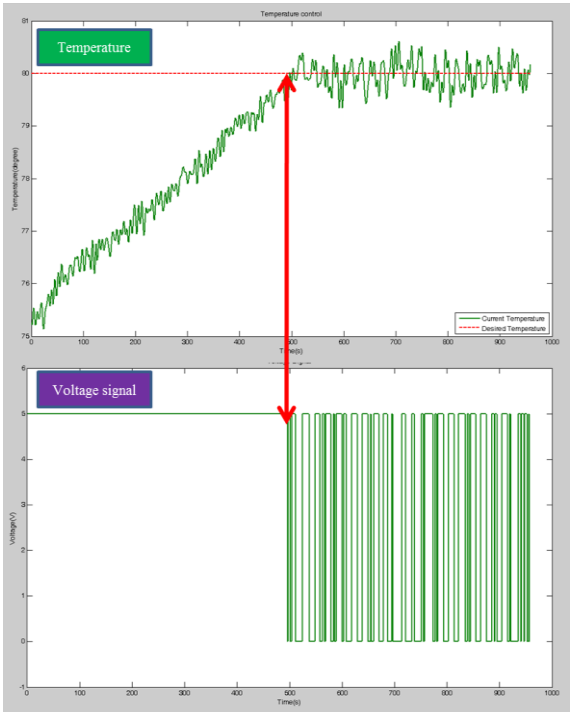

Fig. 6 Temperature control using voltage signals

D. FIBER CHARACTERIZATION

Both random and aligned electrospun PCL microfibers were transferred to loading stubs before carbon coating. The Cressington 208 carbon was used to coat a 3nm thick carbon layer to non-conductive PCL microfiber prior to SEM imaging. The samples were carbon-sputtered two times for 6 seconds at 10^{-4} mbar. The samples were loaded in a Hitachi S-4800 field emission scanning electron microscope. High magnification images were obtained at 1 kV, 5.5 mm and 8.2 mm working distance, to characterize the random and aligned fibers morphologies respectively. The fiber diameters were measured using Quartz-PCI Image Management System®.

E. SEEDING OF CE3 CELLS ON PCL FIBERS SCAFFOLDS

To determine suitability of scaffolds for stem cell culture, CE3 mouse embryonic stem cells (ATCC, USA) were utilized due to their ability to constitutively express green fluorescent protein under the β-actin promoter [23]. These cells were cultured upon mouse embryonic fibroblast feeder layers (Global stem, USA) as previously described to induce embryoid body formation and differentiation [24]. CE3 cells were subsequently removed from feeder layers and cultured in suspension on agar-coated plates in a 4-/4+ treatment protocol with 0.5 µM retinoic acid (Sigma-Aldrich) [18]. Resultant EBs consisted of stem cell aggregates containing a high percentage of neural progenitor cells. Randomly oriented electrospun scaffolds were secured in place on 1.5% agar-coated coverslips and sterilized using ultra-violet radiation for 30 minutes. Select scaffolds were coated with ultra-pure 0.1% gelatin (Millipore, USA) to enhance cell attachment. Individual CE3-derived EBs were removed from suspension and placed on sterilized scaffolds. EBs were cultured in cell medium without LIF on electrospun scaffolds for 7 days before analysis. Fluorescent images were acquired on a LEICA 3000B inverted microscope using an X-cite series 120Q fluorescent light source (Lumen Dynamics) coupled to a Retiga 2000R fast cooled mono 12-bit camera (Q-imaging).

RESULTS AND CONCLUSION

A. EFFECTS OF NOZZLE DIAMETER

Nozzle diameter decides initial diameter of fibers like direct deposition and diameter of fibers is shrunk by electrical force and gravity force after spinning. Fig. 7 presents analysis of relationship between nozzle diameter and fiber diameter. The fiber diameters were measured using Quartz-PCI Image Management System®. The diameters show from 10µm to 220µm at 80°C when nozzle diameter was increased from 150µm to 1.7mm. Fibers show discontinuous in nozzle diameter 150µm so it is not controllable and expected. Thus, the minimum size of fiber diameter to be controlled and expected is 28µm at 80°C using nozzle diameter 200µm.

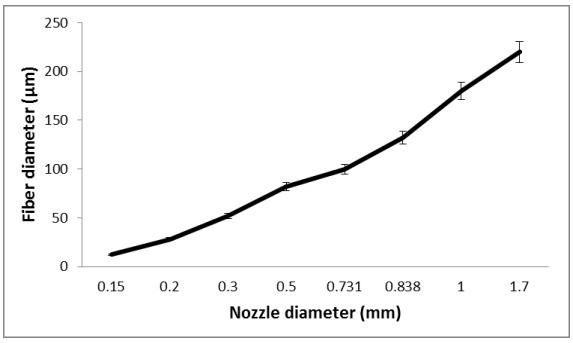

Fig. 7 Analysis of nozzle diameter and fiber diameter

B. EFFECTS OF TEMPERATURE

As shown in Fig. 3, temperature has strong influence on PCL fiber diameter because of changing dynamic viscosity. Fig. 8 (A) represents analysis of temperature and fiber diameter. Chamber that polymers contained are heated by controlled heating pad from 80°C to 120°C. Fiber diameters are slightly increased when temperatures are increased because lower viscosity of polymer at higher temperatures allowed more resins were able to pull from the reservoir increasing fiber diameter. Moreover, speeds of melt electrospinning are changed depended on temperatures. Temperature vs. melt electrospinning speed is an important parameter to control morphology of scaffolds. Table 1 shows fiber weights depended on temperature for 10 minutes using 200μm nozzle. Electrospinning speed (S_f) is calculated by

$$S_f = \frac{w/t}{D} \times \frac{1}{\pi r^2} \quad (1)$$

where, w is weight of fibers, r is fiber radius, t, 600 seconds, is time of electrospinning, and D, 1.145g/cm^3, is density of PCL polymer.

Table1. PCL fiber properties depended on temperatures (spinning time: 10 minutes using 200μm nozzle)

Temperature(°C)	80	90	100	110
Weight(g)	0.1	0.3	0.72	1.18
Fiber diameter(μm)	28	31	33	37

As shown in Fig. 8(B), the speeds are increased when temperatures are increased because of allowing more resins. Based on this result, morphology of scaffolds is able to be controlled variously through x and y axis speed controls.

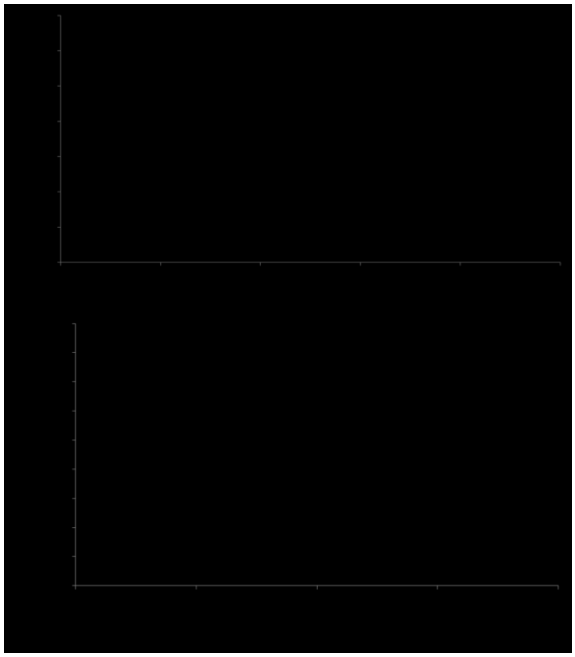

Fig. 8 Analysis of (A): Temperature and fiber diameter and (B): speed of melt electrospinning under various temperatures using 200μm nozzle

C. EFFECTS OF DISTANCE AND VOLTAGE POWER

Fig. 9 shows effects of distance between nozzle and counter electrode and voltage power. As explained in section "Effects of temperature", fiber diameters were increased when temperature was increased from 80°C to 90°C. Distance and voltage power are parameters related to electrical forces. Fiber diameters were decreased if voltage powers were increased while fiber diameters were increased if distances were increased. In terms of parameters rate, fiber diameters show approximately 2 times increase when distance are increased to double. When voltages are increased to double, fiber diameters show approximately 2 times decrease. This result is content with Coulomb's law, Eq.2, in electric field force from a point.

$$F_e = -q\frac{\Delta\phi}{d} \quad (2)$$

where, F_e is electrical field force, q is charge, $\Delta\phi$ is the potential difference between the plate and point, and d is the distance.

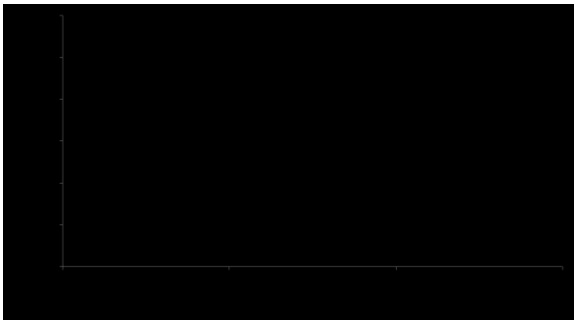

Fig. 9: Effects of distance and voltage power using 200μm nozzle

D. SEEDING OF CE3 CELLS ON PCL FIBERS SCAFFOLDS

The ability of these microfiber scaffolds to serve as a bioengineering substrate was examined through cell seeding experiments (Fig. 10). In panel A, cell seeding experiments showed undirected rapid proliferation and differentiation of the ESC-derived neural progenitors when plated in a controlled 2D environment. Fiber directed outgrowth from seeded EBs can be observed in Panels B and C. Proliferation slowed significantly when cells were seeded on pure PCL-melt fibers, as shown in panel C; however, rapid proliferation was restored and directed outgrowth retained upon gelatin coating of the microfibers as seen in panel B. Large fiber size and scaffold porosity were overcome through cellular secretion of a secondary extracellular matrix used to bridge large gaps between fibers. Interestingly, a more consistent cellular morphology was also observed in proliferating cells seeded on microfibers, suggesting that the topographical cues were controlling cell behavior when compared to 2D culture. Melt electrospinning microfibers were shown to support and direct CE3 cell proliferation with and without a gelatin coating, and can thus be seen as a suitable tissue engineering tool.

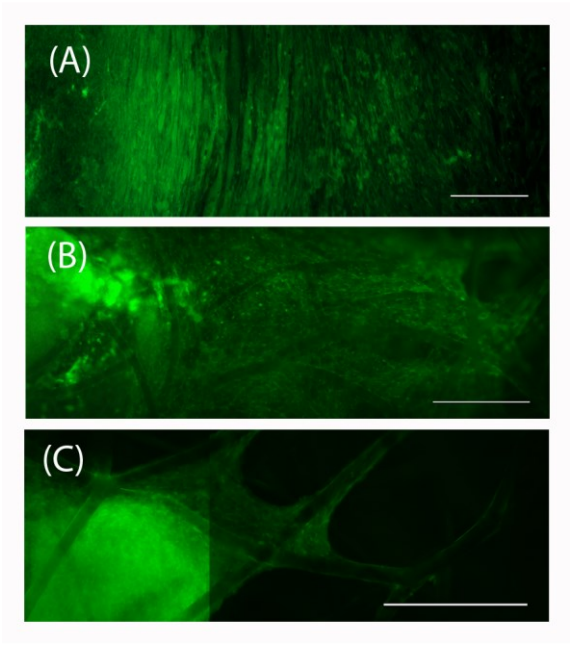

Fig. 10 Murine CE3 Embryoid Bodies were cultured for 7 days on glass coated in 0.1% gelatin (A), randomly aligned melt-electrospun fibers coated in 0.1% gelatin (B), and randomly aligned non-coated melt-electrospun fibers (C). Cells were cultured at 37°C in 0.5% CO2. Images were taken using a LEICA DMI 3000B fluorescent microscope and coloured using Q-capture imaging suite. Fiber diameter varied from 70-90 µm. Scale bars represent 500µm.

CONCLUSION

In this study, all significant parameters involved with fiber diameter and morphology of scaffold in melt electrospinning are investigated. Due to the custom-made nozzles, the initial diameter of fibers becomes restricted so various diameters of fibers could be fabricated by melt electrospinning technique. Moreover, PCL polymer's behavior was learned from analysis of "effects of temperature" and Coulomb's law in electric field force from a point was verified by analysis of "effects of distance and voltage power. Based on these results, we fabricated controlled morphology of scaffolds and successfully cultured CE3 mouse embryonic stem cells on the fabricated scaffold. In our follow up studies, we will make modeling of melt electrospinning based on our results and fabricate controlled 3D scaffolds.

REFERENCES

[1]M.E. Gomes, R.L. Reis, "Tissue engineering: Key elements and some trends," Macromolecular Bioscience, 2004; 4(8): p. 737-742.

[2]R. Langer, J. P. Vacanti, "Tissue Engineering," Science, 1993; 260(5110): p. 920-926.

[3]R.C. Thomson, M.C. Wake, M.J. Yaszemski, A.G. Mikos, "Biodegradable polymer scaffolds to regenerate organs," Biopolymers Ii, 1995; 122: p. 245-274.

[4]A.S. Goldstein, G.M. Zhu, G. E. Morris, R. K. Meszlenyi, A.G. Mikos, "Effect of osteoblastic culture conditions on the structure of poly(DL-lactic-co-glycolic acid) foam scaffolds," Tissue Engineering, 1999; 5(5): p. 421-433.

[5]J. Ko, K. Kolehmainen, F. Ahmed, M.B.G. Jun, S.M. Willerth, "Towards high throughput tissue engineering: development of chitosan-calcicum phosphate scaffolds for engineering bone tissue from embryonic stem cells," *Am J Stem Cell*, 2012; 1(1).

[6]A.G. Mikos, J.S. Temenoff, "Formation of highly porous biodegradable scaffolds for tissue engineering," *Electron J Biotechnol*, 2000; 3(2): p. 6.

[7]D.T. Mooney, C.L. Mazzoni, C. Breuer, K. McNamara, D. Hern, J.P. Vacanti, R. Langer, "Stabilized polyglycolic acid fibre based tubes for tissue engineering," *Biomaterials*, 1996;17(2):p. 115-124.

[8]Y.S. Nam, J.J. Yoon, T.G. Park, "A novel fabrication method of macroporous biodegradable polymer scaffolds using gas foaming salt as a porogen additive," *Journal of Biomedical Materials Research*, 2000;53(1):p. 1-7.

[9]K. Whang, C.H. Thomas, K.E. Healy, G. Nuber, "A Novel Method to Fabricate Bioabsorbable Scaffolds," *Polymer*, 1995;36(4):p. 837-842.

[10] S. Shukla, E. Brinley, H.J. Cho, S. Seal, "Electrospinning of hydroxypropyl cellulose fibers and their application in synthesis of nano and submicron tin oxide fibers," *Polymer*, 2005;46(26):p. 12130-12145.

[11] P.D. Dalton, K. Klinkhammer, J. Salber, D. Klee, M. Moller, "Direct in vitro electrospinning with polymer melts," *Biomacromolecules*, 2006;7(3):p. 686-690.

[12] J.S. Kim, D.S. Lee, "Thermal properties of electrospun polyesters," *Polymer Journal*, 2000;32(7):p. 616-618.

[13] L. Larrondo, R.S.J. Manley, "Electrostatic Fiber Spinning from Polymer Melts .2. Examination of the Flow Field in an Electrically Driven Jet," *Journal of Polymer Science Part B-Polymer Physics*, 1981;19(6):p. 921-932.

[14] L. Larrondo, R.S.J. Manley, "Electrostatic Fiber Spinning from Polymer Melts .3. Electrostatic Deformation of a Pendant Drop of Polymer Melt," *Journal of Polymer Science Part B-Polymer Physics*, 1981;19(6):p. 933-940.

[15] L. Larrondo, R.S.J. Manley, "Electrostatic Fiber Spinning from Polymer Melts .1. Experimental-Observations on Fiber Formation and Properties," *Journal of Polymer Science Part B-Polymer Physics*, 1981;19(6):p. 909-920.

[16] S. Lee, S.K. Obendorf, "Developing protective textile materials as barriers to liquid penetration using melt-electrospinning," *Journal of Applied Polymer Science*, 2006;102(4):p. 3430-3437.

[17] J. Lyons, C. Li, F. Ko, "Melt-electrospinning part I: processing parameters and geometric properties. *Polymer*, 2004;45(22):p. 7597-7603.

[18] S.H. Park, T.G. Kim, H.C. Kim, D.Y. Yang, T.G. Park, "Development of dual scale scaffolds via direct polymer melt deposition and electrospinning for applications in tissue regeneration," *Acta Biomaterialia*, 2008;4(5):p. 1198-1207.

[19] P.D. Dalton, D. Grafahrend, K. Klinkhammer, D. Klee, M. Moller, "Electrospinning of polymer melts: Phenomenological observations," *Polymer*, 2007;48(23):p. 6823-6833.

[20] G. Kim, J. Son, S. Park, W. Kim, "Hybrid Process for Fabricating 3D Hierarchical Scaffolds Combining Rapid Prototyping and Electrospinning," *Macromolecular Rapid Communications*, 2008;29(19):p. 1577-1581.

[21] T.D. Brown, P.D. Dalton, D.W. Hutmacher, "Direct Writing By Way of Melt Electrospinning," *Advanced Materials*, 2011;23(47):p.5651.

[22] M.A. Woodruff, D.W. Hutmacher, "The return of a forgotten polymer-Polycaprolactone in the 21st century," *Progress in Polymer Science*, 2010;35(10):p. 1217-1256.

[23] L.D. Adams, L. Choi, H.Q. Xian, A.Z. Yang, B. Sauer, L. Wei, D.I. Gottlieb, "Double lox targeting for neural cell transgenesis," *Molecular*

Brain Research, 2003;110(2):p. 220-233.

[24] G. Bain, D. Kitchens, M. Yao, J.E. Huettner, D. I. Gottlieb, "Embryonic Stem-Cells Express Neuronal Properties in-Vitro," *Developmental Biology*, 1995. 168(2): p. 342-357.